IL NUOVO CIMENTO **39 C** (2016) 313
DOI 10.1393/ncc/i2016-16313-y

COLLOQUIA: La Thuile 2016

AMS02 results after 4 years of data taking on the International Space Station

M. INCAGLI on behalf of the AMS02 COLLABORATION
INFN, Sezione di Pisa - Pisa, Italy

received 26 July 2016

Summary. — The AMS02 experiment is taking data on the International Space Station since May, 19, 2011. This report summarizes the key results published or presented in public conferences using the data collected in the first 4 years of the mission, trying to interpret them in terms of the latest models of Cosmic Ray (CR) propagation. In particular the fluxes of primary CR, like proton, Helium and Carbon, or of secondaries like Lithium and Boron, can be used to constraint the models and compare them with the observed anti-proton flux, to see if hints of Dark Matter (DM) can be identified. The same can be done in the lepton sector by looking at electrons and positrons. In the near future AMS02 will continue the observation of light nuclei, including isotopes like Deuterium, He-3 and He-4, and of anti-nuclei, like anti-Deuterium and anti-Helium, which represent, together with anti-protons and positrons, the golden channels in which to look for eventual Dark Matter or antimatter signals.

1. – Introduction: the physics of charged cosmic rays

The main goal of AMS02, on the International Space Station (ISS), is to study charged Cosmic Rays (CR) in the energy range between 1 GeV and few TeV. The flux of charged cosmic rays, shown in fig. 1 has been studied, and is being studied, by many experiments in a wide range of energies, approximately from 10^{12} GeV to 10^{20} GeV, and in a range of fluxes which spans 20 orders of magnitude. Due to this huge span, many different techniques are used which require larger and larger surfaces covered as the energy grows.

In particular, due to technical limits in mass and dimensions and to the large cost, experiments mounted on satellites outside the atmosphere are limited to energies of few to few hundreds of TeV, depending on particle type. While this is a limit with respect to ground, experiments in space are sensitive to the primary CR component, *i.e.* before interacting with the atmosphere, which allows them to accurately measure the nuclear charge (Z) and, if equipped with a magnet, to measure the sign of the charge identifying the anti-particle component of CR.

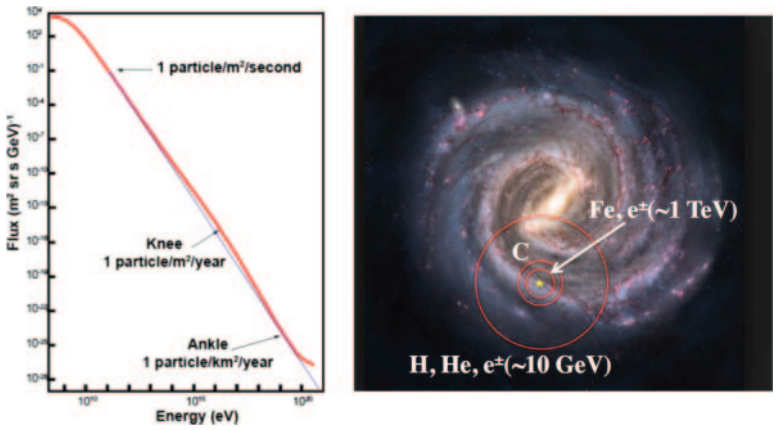

Fig. 1. – Left: integrated flux of charged cosmic rays as a function of the particle energy. Right: region of the galaxy from which the different particles can reach the Earth.

The presence of the magnet is a key element that separates Magnetic Spectrometers from Calorimetric Experiments. In fact, while it gives access to anti-particles, its presence limits the field of view, and thus the geometrical acceptance, of the instrument. This is relevant as the flux of CR drops down very rapidly with energy, as shown in fig. 1 As an example, fig. 2 shows a qualitative comparison of the Field of Views observed by AMS02 and by Fermi.

For what regards charged cosmic rays, due to the limited energy range covered, space experiments can probe only the local galaxy. In particular high-Z elements interact with the local Intestellar Medium producing lighter elements (*e.g.* C $\rightarrow$ B). Electrons, instead lose energy via Inverse Compton scattering and via synchroton radiation, both of which strongly depend on the energy of the particle. As a consequence, high-Z elements and

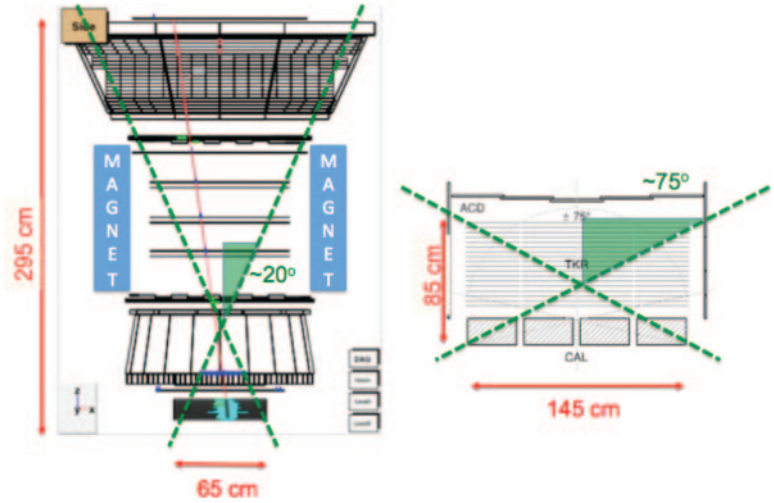

Fig. 2. – Proton rejection power at 90% signal efficiency with TRD detector.

TeV electrons are locally produced and their spectra can be distorted by the presence of nearby sources. This is shown in fig. 1 in which the region of the galaxy probed by different components of the CR flux is pictorially represented.

2. – The physics of AMS

AMS-02 has taken data for 4 years and is expected to be operative on the ISS for twice as much, gathering a huge amount of data and determining long term variations of the cosmic rays fluxes and composition, from protons to iron, and over a wide energy range. These data will improve our understanding of the interstellar propagation and of the mechanisms at the origins of cosmic rays. Moreover, knowledge of "standard" cosmic rays is necessary to determine the background to an eventual additional component due to self-interaction of WIMP type Dark Matter candidates.

Dark Matter makes up $\simeq 80\%$ of the mass of the Universe but, up to now, only gravitational evidence of its existence has been observed. Although the energy scale at which this particle can be found is not known, there is an interesting convergence of hints which point to the so-called *Weakly Interacting Massive Particle* (WIMP), a particle in the mass range few GeV to few TeV undergoing weak interactions. A Wimp could self-annihilate producing pairs of Standard Model particles which increase the fluxes observed at earth with respect to the one produced by standard CR. This is known as *Dark Matter indirect search*. In particular the fluxes which would eventually undergo the largest relative modification are the rarer ones, and in particular the fluxes of anti-particles, like positrons, anti-protons and, eventually, anti-deutirium and anti-helium nuclei.

The existence of large domains of antimatter in the universe is still an open question although nowadays there is growing experimental evidence of the non- existence of stars and galaxies made entirely of antimatter. The best way to show the evidence of an antistar is obviously the detection of antimatter with $Z \sim 2$. This will be one of the tasks of AMS.

3. – The AMS-02 Detector

The AMS-02 detector consists of nine planes of precision silicon tracker, with 6 planes of the inner tracker located inside the bore of a permanent magnet, a transition radiation detector (TRD), four planes of time-of-flight counters (TOF), an array of anti-coincidence counters (ACC) surrounding the inner tracker, a ring imaging Cherenkov detector (RICH) and an electromagnetic calorimeter (ECAL).

For a detailed description of the detector see [1] and references therein. Here only the parameters relevant for the different analyses will be described. In particular, the TRD and ECAL capabilities of discriminating positrons from protons, the tracker capability in determining the charge sign and the charge (Z) resolution of the various subdetectors will be shortly discussed.

3˙1. *ep rejection.* – There are three main detectors which allow for a significant reduction of the tremendous proton background in the positron and electron samples, the so-called *ep rejection*. These are the TRD, the ECAL standalone and the ECAL in conjuction with the tracker through the comparison of the independent measurements of energy and momentum (E/p ratio).

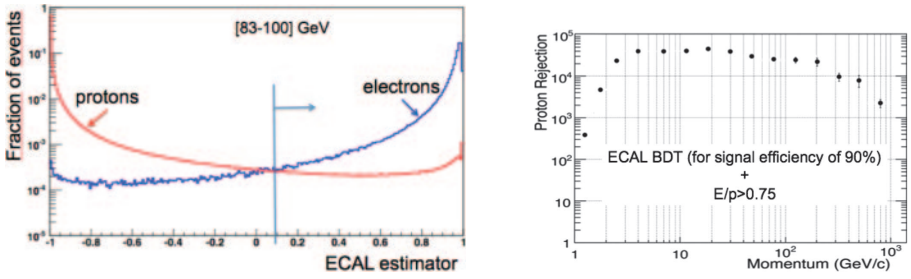

(a) (b)

Fig. 3. – a) ECAL estimator for 100 GeV electrons and protons selected by TRD and tracker sign. b) Proton rejection for a combined cut on ECAL estimator and on $E/p > 0.75$ (energy-momentum matching).

The TRD measures the transition radiation which is emitted by relativistic particles when crossing boundaries between materials having a different dielectric constant [2].

The discrimination between electrons and protons in ECAL is based on the different characteristics of electromagnetic and hadronic showers. A set of variables which describe the shower development, like the transversal width, the number of hits, the fraction of energy per layer, etc., are combined together by means of a multivariate analysis in order to provide the ECAL estimator shown in fig. 3(a). The statistical technique used for combining the input variables into a single estimator is the Boosted Decision Tree (BDT) [3].

In addition, leptons and hadrons can be discriminated by the ratio E/p, where E is the energy measured by the ECAL and p the momentum measured by the tracker. By combining a cut on the ECAL BDT at 90% efficiency on the signal with a cut on $E/p > 0.75$, the *ep* rejection of fig. 3(b) is obtained. When combined with the TRD rejection, the required *ep* rejection of 10^5–10^6 is reached.

3˙2. *Charge confusion.* – A fraction of charged events, depending on the particle momentum, are wrongly reconstructed as positive tracks being negative and viceversa. There are two effects which can induce charge confusion (CC). The first one is the finite tracker resolution in measuring the rigidity R of the track, shown in fig. 4(a). This effect, called *spillover*, is parametrized and it turns out to be negligible at 400 GeV, as measured at the Test Beam performed before the flight, while at $E = 1$ TeV it is 2%.

The second effect is the production of secondary tracks along the particle path, due to interactions with the $0.6X_0$ of the detector material above ECAL. These secondary tracks create additional hits close to the ones produced by the main particle; as a consequence a CC due to *wrong hits association* can be induced. This effect can be quantified by building a *tracker estimator* very similar to the one used for ECAL. It is built by using a set of input variables which are sensitive to the layer activity: number and distance from the main track of the hits in each tracker plane, χ^2 of the track fit, number of hits in TRD, etc. These variables are combined by the BDT technique in a single classifier, which has been tested on Test Beam data, where the correct track sign is known. A good agreement of the classifier between data and Montecarlo (MC) is observed as shown in fig. 4(b), which allows us to use MC to determine the fraction of CC events as a function of energy.

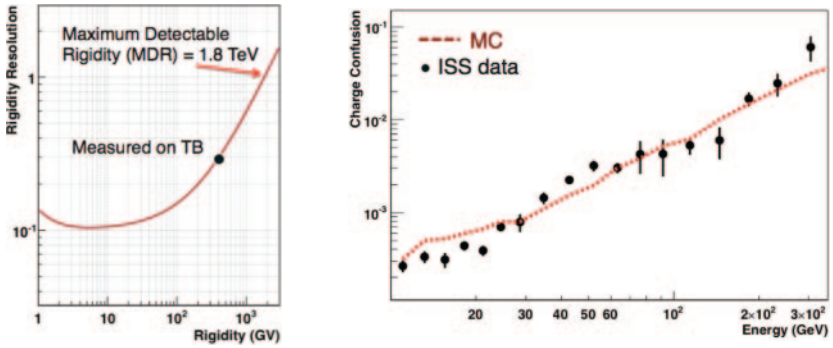

(a) (b)

Fig. 4. – a) Tracker rigidity resolution on protons. b) Charge Confusion due to wrong hit association.

3˙3. *Z reconstruction.* – The value of the nuclear charge Z of incoming particles is measured, in AMS, by many subsystems. The first tracker layer plane, on the top of the detector, determines the charge by the $\mathrm{d}E/\mathrm{d}x$ released in the silicon. The same technique, but with different materials, is used in TRD —energy loss in Xe/CO_2 gas mixture— and in the TOF —two layers of plastic scintillators. The RICH, instead, determines Z by the number of photons in the Cherenkov ring. Figure 5 shows the AMS Z-determination power for the different subsystems for charges up to Oxygen.

4. – Results

4˙1. *Proton and Helium flux.* – The most abundant CR components are Hydrogen and Helium nuclei. Their spectra are shown in fig. 6 as a function of Rigidity (R) multiplied by the standard factor $R^{2.7}$. Both spectra show an evident feature, *i.e.* a deviation from a simple power law with a (soft) break at approximately the same value of R: 200–300 GeV. Moreover, their local spectral index, *i.e.* the index $\gamma(R)$ obtained by fitting 4 or 5 consecutive and non overlapping Rigidity bins, is very similar with a shift of $\simeq 0.1$ in a large energy range (see fig. 7).

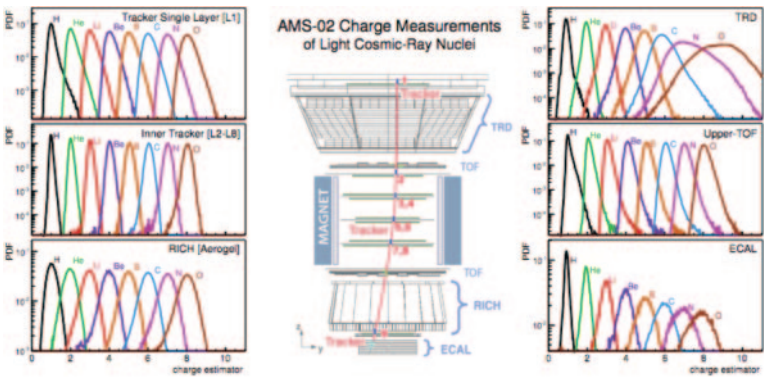

Fig. 5. – AMS Z reconstruction capability.

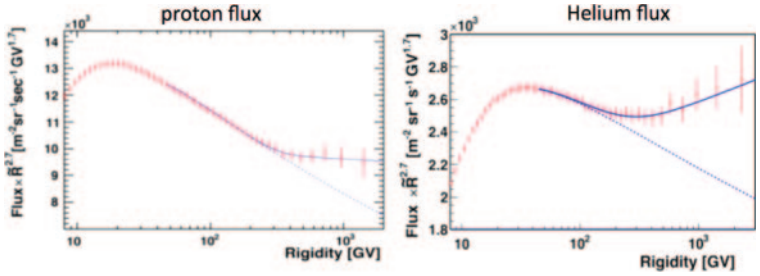

Fig. 6. – Proton and Helium fluxes, multiplied by the standard factor $R^{2.7}$. Superimposed is a fit to guide the eye and show the break in the energy spectrum.

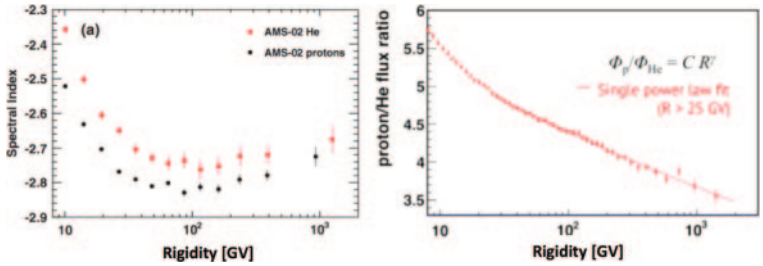

Fig. 7. – Proton and Helium spectral indeces (left) and fluxes ratio (right).

The fact that the p/He spectrum is featurless, as shown in fig. 7, seems to indicate that the same mechanism is at work both for protons and Helium nuclei. There are several possible reasons which can explain this fact, and they have been discussed in several papers (see, *e.g.*, [5]): acceleration in Supernovae Remnants, propagation in the Interstellar Medium, presence of local or distant sources. To discriminate among different possibilities, more informations have to be collected from different nuclear species. AMS02 is in the condition of providing accurate measurements both of primary and of secondary species within the same instrument. Lithium and Boron, for example, are secondary species, *i.e.* produced by the interaction of primary cosmics rays, like Carbon or Oxygen, in the interaction with the interstellar medium. Figure 8 shows the Lithium flux and the ratio of Boron to Carbon (B/C) nuclei.

In Lithium flux a break at a Rigidity value similar to the p and He one is observed. A possible explanation is that a component of primaries and secondaries are accelerated together inside a Supernova Remnant shock wave. If this is the case, a similar break would be expected also in Carbon, although not necessarely at the same Rigidity. The ratio B/C, however, doesn't show any particular feature, so it will be necessary to look at the single fluxes in order to have additional clues on the details of the mechanisms of production and acceleration of CRs in the galaxy.

4˙2. *Electrons and positrons.* – A channel which is of particular interest in the search for DM is the positron one. It has been suggested since long [4] that an e^+e^- pair can be produced by DM annihilation thus increasing the positron flux with an additional component which is essentially monochromatic at the source. Electrons and positrons then travel through the galaxy, eventually reaching the earth, losing their momentum

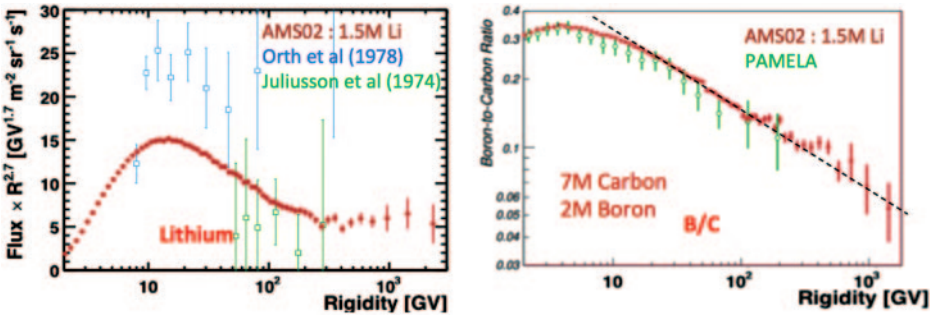

Fig. 8. – Left: Lithium flux. Right: B/C flux ratio.

by interacting with the Interstellar Medium and with the galactic magnetic field. As a result, the positron flux should show an increase, with respect to standard propagation, and then a sudden drop at a threshold which coincides with the DM mass.

An increase with respect to the expected secondary positron production has been first clearly observed by Pamela experiment [6] in the positron fraction $e^+/(e^+ + e^-)$, and confirmed with high precision by AMS02 (see fig. 9, from [7]). AMS02 has also extended the measurement up to energies of 500 GeV showing, for the first time, a flattening of the spectrum. However, no clear sign of drop in the fraction has been yet observed.

AMS has also measured separately and with great accuracy the single fluxes, shown in fig. 10, after multiplying for the standard E^3 factor, observing some unexpected features. Both fluxes show a break in the spectrum at 30 GeV, while, contrary to protons and Helium which, as electrons, are a primary component of the Cosmic Rays no structure is observed for the electrons at 300 GeV. The statistical error on positron flux does not allow to reach a firm conclusion about positrons, which are a secondary species, like Lithium, about the presence of such a break at 300 GeV. The reason of the break at 30 GeV, at an energy which is 10 times smaller than for protons and Helium, is not yet clear. The other unexpected feature is that the electron and positron spectral index, above 20 GeV, is very much the same, with a shift of 0.5 (fig. 10).

These features cannot be described by the standard propagation of CRs and require the introduction of an additional primary source of e^+e^- pairs. A strong candidate for this role, already proposed many years ago [8], is the population of local (*i.e.* less than 1 kPc away) pulsars, *i.e.* fastly spinning neutron stars in which e^+e^- pairs are produced

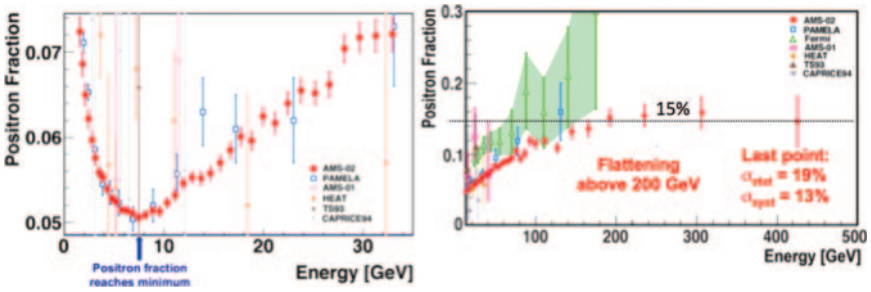

Fig. 9. – Positron fraction. Left: low energies. Right: high energies.

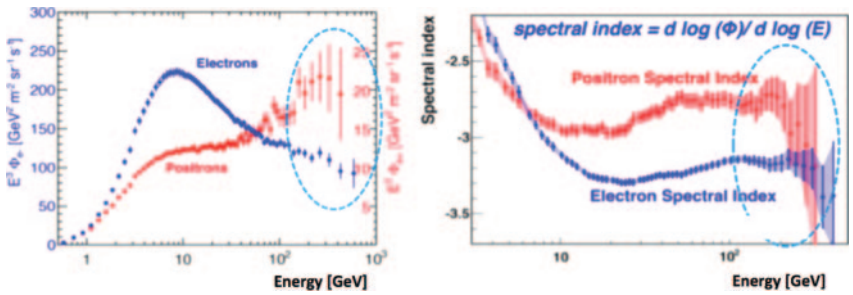

Fig. 10. – Electron and positron fluxes and spectral indeces. The circled regions represent the energy range in which Proton, Helium and Lithium fluxes show the break.

by the interaction of energetic photons in the strong magnetic field surrounding the stars (more detail in [9]). This mechanism does not produce protons, or light nuclei, therefore it can explain the particular behaviour of electrons and positrons. Also ee pairs produced in pulsars are expected ti have a cutoff energy, so a drop in the positron fraction is expected, however each pulsar has its own cutoff value therefore the overlap of several such structures results in a drop which is expected to be smoother with respect to the one caused by DM interaction. AMS02 will be able to explore up to 1 TeV the positron fraction.

4˙3. *Anti-protons.* – While the excess of positrons can be explained with the Pulsar mechanism, this does not work for anti-protons, therefore it is important to look at the similar plot in the $\bar{p}/p$ ratio. Note that in this case the ratio is $\simeq 10^{-4}$, thus it essentially coincides with the fraction $\bar{p}/(p+\bar{p})$.

The anti-proton ratio is shown in fig. 11; it does not show the rise observed in positron fraction, however the spectrum is flatter than expected before AMS02. For example, fig. 11.*right* shows the ratio expected [10] when fitting the model on Pamela data. An excess at energies above 100 GeV is clearly observed. However, once AMS02 data on B/C are taken into account, the models can be re-evaluated and AMS02 data are now much more in agreement with the "predictions" (or, rather, "postditions"). Three examples are shown in fig. 12. Note, however, that although an excess cannot be claimed, by shrinking the error with more data, and by pushing the measurement at higher energies, models

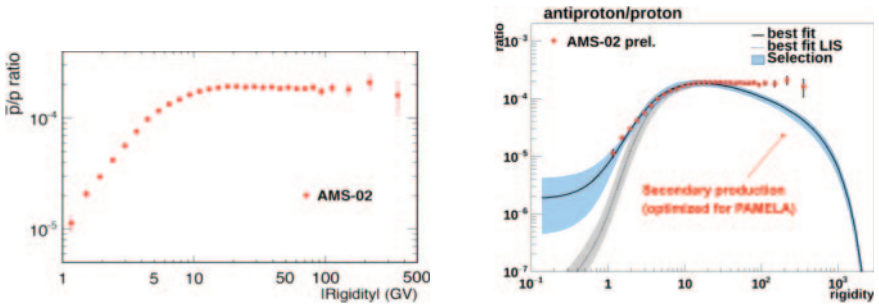

Fig. 11. – Ratio of the fluxes of anti-protons and protons. On the right the ratio is compared with a model of secondary production optimized for Pamela data [10].

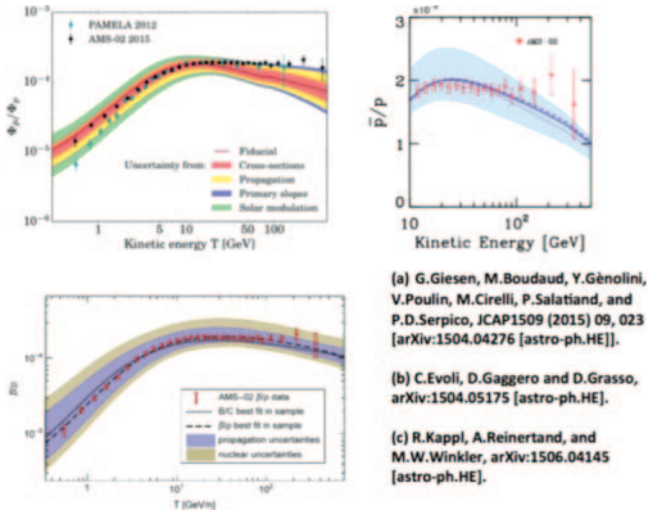

Fig. 12. – Fit of AMS02 $\bar{p}/p$ based on AMS02 B/C ratio (see text for details).

will be challenged again. Unfortunately AMS02 is almost at the limit, in Rigidity, of its capability of separating antiprotons for the much more abundant proton background. The current upper edge of the last bin is $R = 450\,\mathrm{GeV}$; maybe this limit can be pushed to 600 GeV, it will be very hard to go above.

5. – Conclusions

As of now, there is no clear indication, nor need, of a WIMP-like DM component to explain the fluxes observed by AMS02. However the production, acceleration and propagation in the ISM mechanisms of "standard" CRs still have many free parameters which can be adapted to describe single fluxes. The new challenge which AMS02 is setting is to reproduce all the very precisely measured fluxes and ratios at the same time with a coherent set of parameters. As more measurements will come out, on more nuclei as well as on isotopes, like Deuterium, Helium 3 and Helium-4, possibly Berillium-9 and Berillium-10, and the electron fluxes will be extended to higher energies, a precise picture will emerge which will constraint the CR acceleration and propagation models and will eventually allow to show deviations from such models. Additional space missions, like Calet and Dampe, already taking data, and IssCream, which will soon be launched, will contribute to establish this picture.

However, AMS02 unique prerogative will be to improve the current data on anti-particles: positrons and anti-protons but also anti-deutirium and anti-helium. These will be the golden channels in which to look for Dark Matter (or antimatter) signals.

REFERENCES

[1] AMS Collaboration (Accardo L. *et al.*), *Phys. Rev. Lett.*, **113** (2014) 121101.
[2] Luebelsmeyer K. *et al.*, *Nucl. Instrum. Methods Phys. Res., Sect. A*, **654** (2011) 639.
[3] Byron P. R. *et al.*, *Nucl. Instrum. Methods A*, **543** (2005) 577.
[4] Turner M. S. and Wilczek F., *Phys. Rev. D*, **42** (1990) 1001.

[5] Vladimirov A. *et al.*, *Astrophys. J.*, **752** (2012) 68.
[6] Pamela Collaboration, *Nature*, **45B** (2009) 607.
[7] AMS Collaboration (Accardo L. *et al.*), *Phys. Rev. Lett.*, **113** (2014) 121101.
[8] Harding A. K. and Ramaty R., in *20th Int. Cosmic-Ray Conf.*, Vol. **2** (Nauka, Moscow, 1987) 92.
[9] Buesching I. *et al.*, *Astrophys. J.*, **78** (2008) L39.
[10] Dissertation/PhD Thesis Simon Kunz (2014), IEKP-KA/2014-20, `http://ekp-invenio.physik.uni-karlsruhe.de/record/48605`.